



## FIV of PWR fuel rods under local jets : instability threshold and influence of jet configuration

**Boulanger P.<sup>(1)</sup>, Fardeau P.<sup>(1)</sup>, Rigaudeau J.<sup>(2)</sup>**

*(1) CEA, France*

*(2) Framatome, France*

### ABSTRACT

We present an experimental study devoted to fluid-structure interaction on a scale- $\frac{1}{2}$  mock-up, intended to simulate the complex mixed axial-cross-flow representative of PWR core flows in the baffle jetting context. Despite its reduced size, the mock-up retains the overall structure of a PWR fuel assembly. Rod vibratory velocity and flow velocity field were measured by laser techniques. The experimental study demonstrates the validity of fluid-elastic criteria proposed for different grid-to-rod restraining conditions, jet configuration and location.

### INTRODUCTION

Baffle jetting can induce large vibratory amplitudes of fuel rods and thus failure from fretting wear. The pressure difference generating the jets and therefore their intensity have been notably reduced by the up-flow configuration in the core barrel (either initial reactor design or from up-flow conversion). Yet fuel rod support designs have to be justified with respect to baffle jetting, allowing for a possible increase in baffle gaps, or for relatively large gaps resulting from significant pressure loads on the baffles, in the down-flow configurations before conversion. Also, fuel rods should withstand the jets from the blowdown relief holes.

Baffle jetting interaction is related to the vibratory phenomena of circular cylinders subjected to both axial and cross-flow. Uniform cross-flow induced vibrations applied to heat exchanger tube bundle vibrations were extensively investigated and the vibration mechanisms are now well understood [1] [2] [3]. In the case of fuel assembly baffle jetting induced vibrations, two main differences appear. On the one hand, cross-flow is not extended but jetted from a local vertical narrow gap and may be non uniform. The shape of the jet and its location with respect to tube bundle prove to have a great influence. On the other hand, fuel assemblies are not exclusively excited by a cross-flow but also by the main axial-flow of the reactor coolant.

Local cross-flow induced vibrations were studied in [4]. It was shown that vibration mechanisms are very similar to those observed in uniform cross-flow. But additional vibration mechanisms can appear which are related to the small width of the jet. The jet position proves to have a major influence on vibratory amplitude. It was proved that when rod arrays are subjected to both cross-flow and uniform steady axial-flow, a fluid-elastic instability can occur, although the axial-flow tends to stabilize the tube array vibrations.

This paper deals with an experimental study carried out to determine the instability threshold for fuel rod arrays subjected to mixed axial cross-flow. The cross-flow in question is jetted

from a vertical narrow gap simulating baffle jets. In the first part, we describe the experimental test facility and test parameter range. The second part is devoted to vibration signal analysis, instability threshold definitions are covered in part three. Experimental FIV results and instability threshold validation are presented in the final part.

## PART 1 : EXPERIMENTAL TEST FACILITY

An experimental program on mixed axial cross-flow has been undertaken in the CEA CHRISTINE test loop in collaboration with FRAMATOME. Tests have been designed to achieve a reasonable balance between representativity and analytical interpretation.

### 1. 1. CHRISTINE Test Loop

The test loop operates under ambient pressure and temperature (up to 0.4 Mpa and 50 °C). Two independent flow lines provide a composed axial-cross-flow. Axial-flow velocity can be adjusted from 0 to 6 m/s, cross-flow velocity ranges from 0 to 4 m/s, depending on the jet width. A cross-flow injector equipped with four equalizing valves adjusts the flow rate and the jet shape.

A removable slit holder is used to change width and jet location parameters. Slits are centered in the mid-span of the mock-up whatever their width. Figure 1 shows the test section of the experimental apparatus.

The mock-up features an 8x8 rod array with 4 guide thimbles, 4 spacer grids and a 1,9 m height. Thus, overall dimensions roughly correspond to scale-1/2, but with rod diameter, pitch and mechanical properties (Zircaloy cladding with UO<sub>2</sub> equivalent density pellets) identical to those of scale one assembly.

Grid spacing and grid cells were chosen to equal scale one rod frequencies and reproduce identical restraining conditions. Mechanical behaviour and fluid excitation are faithfully reproduced.

Three view ports made of plexiglas allow optical measurements to be done. All measurements were performed in a 3X3 fuel rod array in the vicinity of the jets. Rod numbers were chosen as indicated in figure 2.

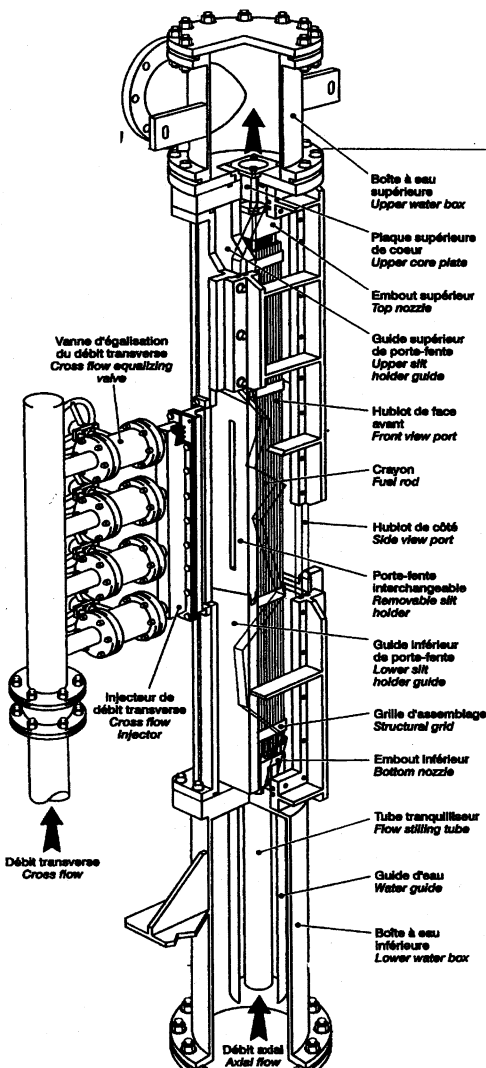


Figure 1 : CHRISTINE Test Section

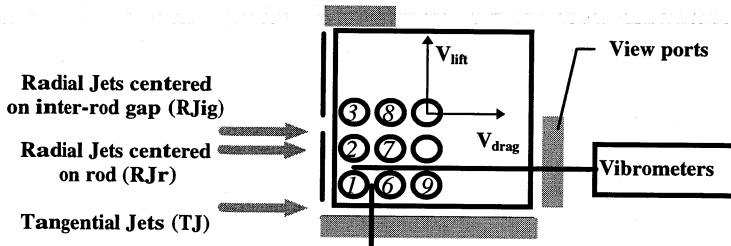


Figure 2 : Rod position and jet direction

### 1.2. Test Parameters

The following chart summarizes the complete experimental program except blowdown hole measurements.

Identification	Jet location	Location (rod number)	Breadth (mm)	Restraining conditions	Axial-flow rate (m <sup>3</sup> /h)
TJ0.5	Tangential	corner rod 1	0.5	type 1	0 - 60 - 90 - 120
TJ5	Tangential	corner rod 1	5	type 1	0 - 60 - 90 - 120
				type 2	0 - 120
				type 3	0 - 120
RJ0.5ig	Radial	Gap between rod 2 and 3	0.5	type 1	0 - 60 - 90 - 120
				type 2	0 - 120
				type 3	0 - 120
RJ0.5r	Radial	Rod 3	0.5	type 1	0 - 60 - 90 - 120
RJ1ig	Radial	Gap between rod 2 and 3	1	type 1	0 - 120
				type 2	0 - 120
				type 3	0 - 120
RJ5r	Radial	Rod 3	5	type 1	0 - 60 - 90 - 120
RJ5ig	Radial	Gap between rod 2 and 3	5	type 1	0 - 60 - 90 - 120
				type 2	0 - 120
				type 3	0 - 120
RJ12r	Radial	Rod 3	12	type 1	0 - 60 - 90 - 120

According to the industrial background of this experimental study, two kinds of slits have been considered, in order to cover a great number of baffle jetting configurations :

- vertical slits which simulate gap between core baffle plates (active height 0.54 m)
- circular holes which reproduce blowdown relief holes.

The paper only deals with vertical slits for which the width ranges from 0.5 mm up to 12 mm. Jets can be radial, centered on rod 3 or centered on the inter-rod gap between rod 2 and rod 3, or tangential, the jet attacking the corner between view port and rod 1. Three kinds of structural grids have been tested :

- type 1 : tight restraining conditions,
- type 2 : moderate restraining conditions,
- type 3 : restraining conditions with small rod/grid stops gap.

## PART 2 : INSTRUMENTATION AND SIGNAL ANALYSIS

### 2.1. Instrumentation

The test loop is equipped with instrumentation monitoring the hydraulic conditions (pressure, temperature and both axial-flow and cross-flow rates). In addition to the loop control instrumentation, the laboratory has developed non intrusive laser measurement techniques.

Rod and grid vibrations are measured by laser vibrometry. The laser device is a single beam Dantec 55XC. The measurement principle is based on Doppler-Fizeau effect : frequency delay of the reflected beam is proportional to the moving target velocity with respect to a fixed source (laser optical head) . Reflecting optical flags are mounted on rods to measure simultaneously, inside the bundle, rod velocity  $V$ , in both orthogonal lift and drag directions ( $V_{\text{lift}}(t)$ ,  $V_{\text{drag}}(t)$  see figure 2).

The mean flow velocity field  $U$  is mapped by laser velocimetry. For laser velocimetry measurements, the mock-up fuel rods are replaced by rigid stainless steel rods. The device used is a 5 Watts Argon-ion gas laser source from which three beams intercept inside the test section (one is the common beam, the two others are called blue and green) giving two fringe patterns of different colors and orientation which represent the measuring volume. Penetration inside the tube bundle and measurement volume dimensions depend on the focal length of the emission lens. To assess realistic flow turbulence properties, a lens with a 160 mm focal length is used, corresponding to a measuring volume about 1 mm long. The back-scattered light of seeding particles passing through the measuring volume is processed with a covariance technique to determine the mean values of two orthogonal velocity components ( $U_{\text{axial}}$  and  $U_{\text{transverse}}$ ), their turbulence fluctuations and their spectral contents.

### 2.2. Signal Analysis

Measurements of rod displacement and velocity were processed to characterize vibratory response and are analysed to detect fluid-elastic instability. Three typical results are computed :

- Velocity Power Spectral Density ( $V_{PSD}$ ) using a classical averaged FFT algorithm.  $V_{PSD}$  peaks represent the rod vibratory frequencies in both lift and drag directions. Velocity locus is a 2D-elliptic representation of the rod motion.
- Displacement Power Spectral Density ( $D_{PSD}$ ) is integrated from the  $V_{PSD}$  .
- Displacement Root Mean Square ( $D_{RMS}$ ) value is computed using Parseval theorem in rod vibration frequency range. Instability graphs represent the variation of  $D_{RMS}$  versus cross-flow rate, for a given axial-flow rate.

Measurements were performed on several rods at different increasing values of axial-flow rate. Figure 3 presents an exemple of instability graphs corresponding to different restraining conditions for a given jet configuration.

Horizontal velocity flow charts are reconstructed from averaged velocity flow measurements for different elevations. Flow rate recirculation areas, vortex, flow distribution around the rods and jet penetration depth provide hints to perform accurate analysis of vibratory responses. Turbulent velocity can be obtained from the standard deviation of the velocity measurement. Spectral analysis is a tool to check the relationship between rod vibratory frequencies and fluid frequencies. Vertical velocity flow charts illustrate the jet profile along the slit.

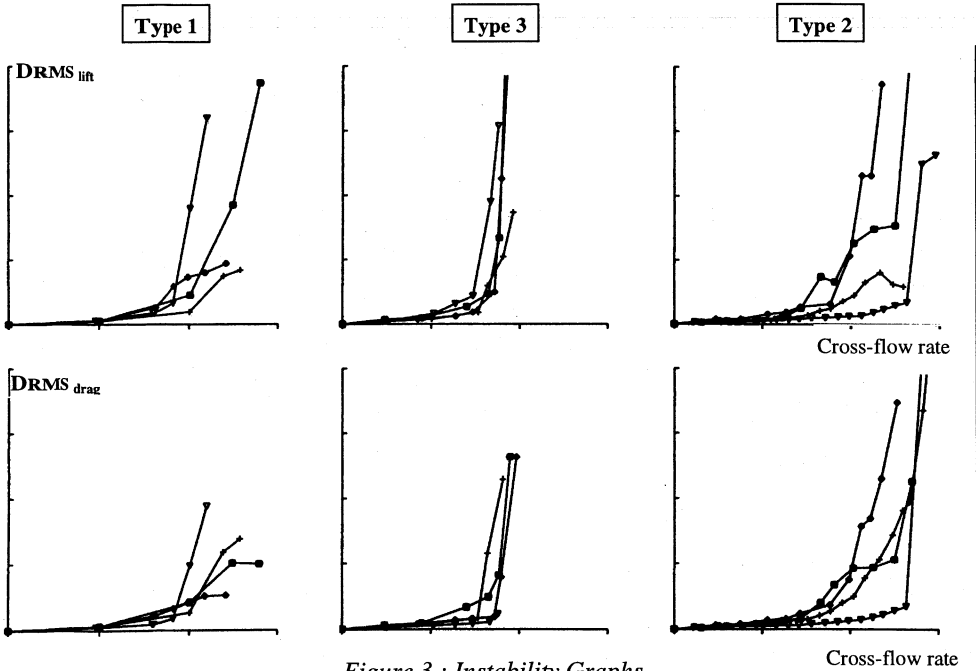


Figure 3 : Instability Graphs

## PART 3 : FLUID-ELASTIC INSTABILITY

### 3.1. Fluid-Elastic Instability Detection

Fluid-elastic instability for circular cylinder bundle subjected to cross-flow is a transition from small-amplitude-uncoordinated vibrations to large-amplitude-combined vibrations. Fluid-elastic instability can be detected by several methods. Four methods were used to estimate instability cross-flow rate :

- an abrupt increase in the vibration amplitude on the instability graph.
- a slight change in vibratory frequencies expressing rod combined motion.
- an abrupt decrease of damping, tending towards zero, which is observed either on  $V_{PSD}$  or  $D_{PSD}$ , showing how much thinner the frequency peak becomes.
- a self-organization of the vibratory displacement displayed by the transition from a random-shaped to an elliptic-shaped velocity locus.

### 3.2. Instability Criteria

Several studies have been undertaken to improve fluid-elastic instability criteria. The first work of CONNORS [1] dealing with uniform cross-flow has been extended to the non-uniform cross-flow [6]. Instability criteria are worked out from the classical stability equation of an elastically mounted rigid cylinder subjected to a fluid-elastic force which is assumed to be proportional to the motion amplitude and the momentum flux of the jet. Then the instability threshold is defined by :

$$\left(hU_{transverse}^2\right)_{effective} = \frac{\int_0^L h(z) U_{transverse}^2(z) \phi_i^2(z) dz}{\int_0^L \phi_i^2(z) dz} = \beta^2 \left(\frac{m_0 \delta_0 D}{\rho}\right) f_i^2$$

The effective value of the momentum flux expresses the influence of the jet profile with respect to the rod mode shape  $\phi_i$ .  $\beta$  is a factor characterizing the jet location, frequency  $f_i$  is the frequency of the rod mode under consideration,  $\rho$  is the fluid density,  $h$  the slit width,  $L$  the total length,  $m_0$  the mass per unit length,  $\delta_0$  the logarithmic decrement characterizing damping. The  $\beta$  factor is set up to typical values from a statistical analysis of a set of experimental results which can be considered as lower bound for available data [7]. From such an approach tangential jets have been considered as more limiting than radial jets.

## PART 4 : RESULTS AND DISCUSSIONS

### 4.1. Axial-Flow-Induced Vibrations

The first results are related to experimental rod frequencies, vibratory levels and vertical jet shape. When the structure is excited by an axial-flow only, whatever the slit configuration may be, rod frequencies measured experimentally are consistent with the ones worked out preliminarily for the three kinds of rod restraining conditions in the grids.

The vibratory level under the single axial-flow excitation is found to be very similar to vibratory levels measured in scale one test loop. The tighter the rod restraining conditions, the smaller the vibratory level. At increasing axial-flow rate rod vibratory levels do not reveal any resonance phenomenon with the axial-flow.

### 4.2. Mixed Axial-Cross-Flow-Induced Vibrations

Fluid-elastic instability was clearly observed in mixed axial cross-flow with at least one of the four detection methods above-mentioned, although not all of them were decisive for each case. Mixed axial cross-flow induced vibration analysis recovers three aspects : before, at and after fluid-elastic instability.

Before instability the increase slope of vibratory levels with cross-flow rate  $D_{RMS} = f(U_{transverse})$  does not seem to significantly depend on rod restraining conditions. The stabilizing effect of axial-flow is noteworthy in some configurations.

When rod are subjected to cross-flow, unexpected instabilities for small cross-flow rates were observed in a few cases. Early large amplitude vibrations have been already investigated [4] in a case of a transverse jet through a narrow gap exciting a tube bundle. Our vibration experimental results show that this phenomenon mainly appears on the rods close to the jet and the PSD frequency peak becomes particularly narrow when approaching the early vibratory level. Such a narrow bandwidth response could be interpreted as a vortex shedding resonance which appears when the frequency of the vortex shedding corresponds to rod frequencies. This specific topic is more extensively presented in [8].

At the instability threshold, combined motion can be observed simultaneously for several close rods in the vicinity of the jet. The vibratory level never exceeds 5 times the vibratory level observed under axial-flow only.

Axial and especially transverse flow velocity fields were found strongly dependent on jet width and location with respect to a rod. At increasing axial-flow rate, the vertical jet shape tends to widthspread in the upper part of the jet. Further, we have noticed a re-entered jet in the lower part of the jet. This typical « plume » effect differs largely from classical uniform and non-uniform cross-flows. In terms of fluid-elastic criteria, this « plume » effect modifies the jet profile influence with respect to the rod mode shape. In addition, rod frequencies can be shifted to higher modes, due to the fact that fluid excitation is spatially located in the upper area of the rod where higher modes are more sensitive.

After fluid-elastic instability, the slope of the instability graph differs according to rod restraining conditions. The increase seems to be more abrupt for tight restraining conditions, leading rapidly to excessive vibratory levels.

#### 4.3. Instability Threshold Validation

If we consider only fluid-elastic instability, a global analysis of vibratory results validates instability thresholds estimation. Figure 4 displays the main results obtained by comparison of experimental momentum flux ( $HU^2_{\text{transverse}}$ ) at instability with criteria previously worked out for different typical jet configuration. Figure 4 is limited to mixed axial cross-flow configuration ( $U_{\text{axial}} = 6 \text{ m/s}$ )

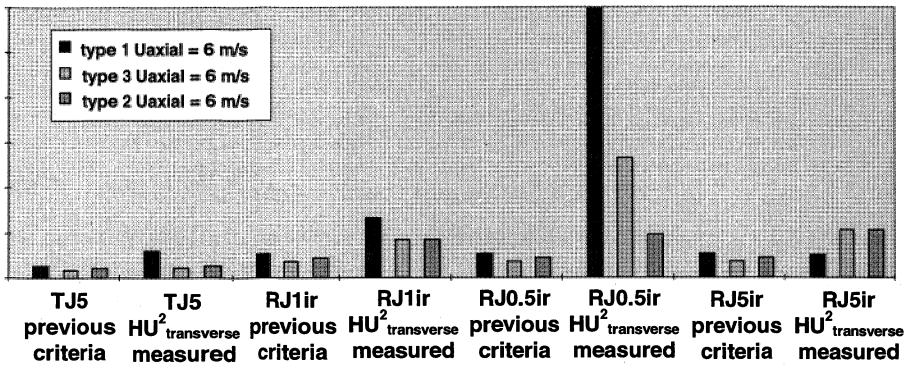


Figure 4 : Comparison of experimental momentum flux at instability and previous criteria

Amongst the baffle jetting configurations that have been examined, tangential jet configuration is found to cause higher vibratory level, for a fixed cross-flow rate. These experimental results tend to confirm the fact that tangential jets are more injurious to life-and-wear than radial jets. As presented above, fluid-elastic instability criteria allow for this situation. Nevertheless some differences can be evidenced for inter-rod radial jet configuration that sometimes tends to increase the vibratory level without overstepping the instability threshold.

Instability threshold levels do not seem strongly dependent on the slit width, thus this approach could be extended to damaged baffle assembly, with notable increase in baffle gaps. Further, the vibratory levels with increasing cross-flow rate observed within the stability range are close to those observed for supply jets located in the bottom of the assembly and for internal core redistribution.

Although fluid-elastic instability criteria were not worked out taking into account either 3D-jet shape or early large amplitude vibrations sometimes encountered, they generally provide thresholds which are found reliable from test and experience feedback.

## CONCLUSION

The presented experimental study covers a large range of test conditions such as jet configuration, jet location, rod restraining conditions and mixed axial cross-flow rate parameters. The analysis provides an extensive data base on baffle jetting interaction which demonstrates the validity of fluid-elastic criteria. This study allows the designer to evaluate conservatism margins available i.e. the difference between design criteria and best-estimate criteria. It also confirms some trends of FIV of PWR fuel rods relevant for realistic applications (damaged baffle assembly).

Nevertheless, margins are desirable because of the great complexity of FIV under mixed axial-flow and local transverse jet, and taking into account scattered results and unexpected behaviour patterns sometimes encountered.

Despite its reduced size, the test loop is able to simulate representative PWR core situations. With slight transformations, the test loop could also reproduce any flow patterns typical of PWR core. The test facility represents a valuable experimental support for mechanical or thermal-hydraulic computer code validation.

## REFERENCES

- [1] Paidoussis M.P. 1983. « A review of flow induced vibrations in reactor and reactor components ». Nuclear Engineering and Design . 74. pp 31-60.
- [2] Connors H.J. 1970. « Fluid-elastic vibration of tube array excited by cross-flow ». In « Flow Induced Vibration in Heat Exchangers ». ed. D.D. REIFF. NY ASME.
- [3] Tanaka H. Takahara S. 1981. « Fluid-elastic vibration of tube array in cross-flow ». Journal of Sound and Vibration. 77. pp 19-37.
- [4] Fujita K. Ito T. Khono N. - 1990. « Experimental study on the vibration of circular cylinders subjected to cross-flow jetted from a narrow gap ». Journal of Fluid and Structure. 4. pp 99-124.
- [5] Connors H.J. 1980. « Fluid-elastic vibration of tube array excited by non-uniform cross-flow ». In « Flow Induced Vibration in Power Plant Component ». PVP 41 - pp 93-107. NY ASME.
- [6] P. Boulanger, Y. Jacques, D. Barbier, P. Fardeau, J. Rigaudeau. 1997. « Experimental study of fuel bundle vibrations with rods subjected to mixed axial-flow and cross-flow provided from a narrow gap ». NUTHOS 5 - paper F6 - Beijing - CHINA
- [7] J. Rigaudeau, E. Labarrière, B. Ladouceur. 1997. « Flow-induced vibration analysis for preventing PWR fuel rods from excessive fretting wear ». NUTHOS 5 - paper F2 - April 14-18 - Beijing - CHINA
- [8] Y. Jacques, D. Barbier, P. Boulanger. 1997. « FIV of PWR fuel rods under local jets : resonance amplitude in the stability range ». SMIRT 14 - paper 514 - Lyon - FRANCE.